

Histone H2A Has a Novel Variant in Fish Oocytes 1

Authors: Wu, Nan, Yue, Hua-Mei, Chen, Bo, and Gui, Jian-Fang

Source: Biology of Reproduction, 81(2) : 275-283

Published By: Society for the Study of Reproduction

URL: <https://doi.org/10.1095/biolreprod.108.074955>

BioOne Complete (complete.BioOne.org) is a full-text database of 200 subscribed and open-access titles in the biological, ecological, and environmental sciences published by nonprofit societies, associations, museums, institutions, and presses.

Your use of this PDF, the BioOne Complete website, and all posted and associated content indicates your acceptance of BioOne's Terms of Use, available at www.bioone.org/terms-of-use.

Usage of BioOne Complete content is strictly limited to personal, educational, and non - commercial use. Commercial inquiries or rights and permissions requests should be directed to the individual publisher as copyright holder.

BioOne sees sustainable scholarly publishing as an inherently collaborative enterprise connecting authors, nonprofit publishers, academic institutions, research libraries, and research funders in the common goal of maximizing access to critical research.

Histone H2A Has a Novel Variant in Fish Oocytes¹

Nan Wu, Hua-Mei Yue, Bo Chen, and Jian-Fang Gui²

State Key Laboratory of Freshwater Ecology and Biotechnology, Center for Developmental Biology,
Institute of Hydrobiology, Chinese Academy of Sciences, Graduate School of the Chinese Academy of Sciences,
Wuhan, China

ABSTRACT

Histone variants and their modification have significant roles in many cellular processes. In this study, we identified and characterized the histone H2A variant *h2af1o* in fish and revealed its oocyte-specific expression pattern during oogenesis and embryogenesis. Moreover, posttranslational modification of H2af1o was observed that results from phosphorylation during oocyte maturation. To understand the binding dynamics of the novel core histone variant H2af1o in nucleosomes, we cloned ubiquitous gibel carp *h2afx* as a conventional histone control and investigated the dynamic exchange difference in chromatin by fluorescence recovery after photobleaching. H2af1o has significantly higher mobility in nucleosomes than ubiquitous H2afx. Compared with ubiquitous H2afx, H2af1o has a tightly binding C-terminal and a weakly binding N-terminal. These data indicate that fish oocytes have a novel H2A variant that destabilizes nucleosomes by protruding its N-terminal tail and stabilizes core particles by contracting its C-terminal tail. Our findings suggest that H2af1o may have intrinsic ability to modify chromatin properties during fish oogenesis, oocyte maturation, and early cleavage.

early development, embryo, FRAP, histone H2A variant, oocyte development, oocyte maturation, oogenesis, ovary, phosphorylation

INTRODUCTION

Histones are central components of nucleosomes and have vital roles in the transmission of heritable gene expression patterns and in the epigenetic regulation of nucleosome mobility [1]. In eukaryotes, numerous histone variants have been identified from almost all histones [2], and the nucleosome incorporation of histone variants can alter the local chromatin structure to facilitate cellular processes such as transcription or development regulation [3, 4]. Histone H2A

shows the greatest diversity [5], and the known variants, including H2AFZ (previously known as H2A.Z), H2AFX (previously known as H2A.X), H2AFY (previously known as macroH2A), and H2AFB1 (previously known as H2A.Bbd), are involved in many cellular processes [6, 7]. For example, H2AFZ is believed to have significant roles in transcriptional regulation, chromosome structure, DNA repair, and heterochromatin formation [8]. H2AFX appears to prevent aberrant repair of DNA double-strand breaks and is implicated in the dosage-dependent suppression of genomic instability and oncogenic translocation [9]. H2AFY is thought to have an important role in X-chromosome inactivation [10], and its extensive repressing role in gene expression, including a significant role in silencing endogenous retroviruses, has been recently shown [11]. H2AFB1 is a quickly evolving hyper-variable mammalian H2A variant and confers lower stability to nucleosomes [12]. Moreover, destabilization of nucleosomes and unfolding of chromatin fiber have been suggested to facilitate the interaction with different transcription factors, chromatin-modifying enzymes, and polymerases [13].

The biological functions of histone variants are to build specialized nucleosomes and to form distinct chromatin structure for facilitating gene expression in specific cells or at different cell cycle stages by replacing canonical histones. Oocytes are highly specialized cells, and numerous oocyte-specific genes have been identified in vertebrates, including fish [14–16]. Oocyte-specific linker histones have been found in vertebrates and invertebrates, and mouse oocyte-specific *H1foo* is essential for maturation of germinal vesicle-stage oocytes [17]. Recently, Marzluff et al. [18] reported on sea urchin histone gene complement and found a set of five cleavage-stage histone genes expressed in oocytes. However, no oocyte-specific core histone variant has been previously identified, to our knowledge.

Oocytes are unique and highly differentiated cells, and numerous oocyte-specific factors are involved in oocyte growth and maturation [19]. Identification of oocyte-specific genes was recently initiated using subtractive hybridization in fish because of their diversity and particularities of reproduction modes [20, 21]. Oocyte-specific genes, including *zp3* [22, 23], *snx* [24], *clecdc* (c-type lectin domain containing AY157616) [15], *clql4l* (AY662672) [16, 25], *spin1l* (spindling 1-like AY627640) [26], and *snrpc* [27], were identified and characterized from *Carassius auratus gibelio*, a unique polyploid fish with dual reproduction modes of gynogenesis and sexual reproduction [28–30]. Screening of an oocyte-specific core histone H2A variant in fish was also performed [14].

In this study, we characterize the histone H2A variant *h2af1o* and reveal its oocyte-specific expression pattern and phosphorylation modification during oocyte maturation. Moreover, we analyze the mobility of nucleosomes containing H2af1o in living cells by fluorescence recovery after photobleaching (FRAP), a powerful tool to study protein-DNA and protein-protein interactions [31–33].

¹Supported by grants from the National Major Basic Research Program (2004CB117401), the National Natural Science Foundation of China (30630050), the Innovation Project of Chinese Academy of Sciences (KSCX2-YW-N-020), the Open Project of State Key Laboratory of Freshwater Ecology and Biotechnology (2008FB007), and the Innovation Project of Institute of Hydrobiology, Chinese Academy of Sciences (075A011301).

²Correspondence: Jian-Fang Gui, State Key Laboratory of Freshwater Ecology and Biotechnology, Center for Developmental Biology, Institute of Hydrobiology, Chinese Academy of Sciences, Graduate School of the Chinese Academy of Sciences, Wuhan 430072, China. FAX: 86 27 68780123; e-mail: jfgui@ihb.ac.cn

Received: 23 November 2008.

First decision: 13 December 2008.

Accepted: 3 March 2009.

© 2009 by the Society for the Study of Reproduction, Inc.

This is an Open Access article, freely available through *Biology of Reproduction's* Authors' Choice option.

eISSN: 1259-7268 <http://www.biolreprod.org>

ISSN: 0006-3363

TABLE 1. Primers used in this study.

Primer name	Sequence	Usage
<i>h2af1o</i> -1	5'-GAGGTGCTGGAGTTGGCG-3'	Amplify in situ probe
<i>h2af1o</i> -2	5'-AAGCACCAGTCAGTCAAGTGC-3'	
Y5'	5'-GCGAATTCTCTAGATATGTCCGGTCGCGGTAAGAA-3'	<i>h2af1o</i> RT-PCR
Y3'	5'-GGATCCAAGCTTTTAGTCCAGTGCACGAGCGGAGT-3'	
<i>h2afx</i> 5'	5'-GCGAATTCTCTAGATATGTCTGGAAGAGGTAAAACC-3'	<i>h2afx</i> RT-PCR
<i>h2afx</i> 3'	5'-GGATCCAAGCTTTTAATACTCTTGTGATTGAGAAGA-3'	
<i>bactin</i> forward primer	5'-CACTGTGCCCATCTACGAG-3'	Control in RT-PCR
<i>bactin</i> reverse primer	5'-CCATCTCCTGCTCGAAGTC-3'	
1-1*	5'-AGATCTATGTCCGGACGCGGTAAGAAGCT-3'	Plasmid construction for FRAP
1-2*	5'-GAATTCCTCAGTCAAGTGCTCGAGCGGAGTC-3'	
2-1*	5'-AGATCTATGTCTGGAAGAGGTAAAACCGGAGG-3'	
2-2*	5'-GAATCTTAATACTCTTGTGATTGAGAAGAACCCTTCTTTCCC-3'	
3-1*	5'-AGATCTTCCGTGTCGCGTTCGACGC-3'	
4-2*	5'-GAATTCCTCACTTCTTGGGCAGGAGCTGCG-3'	
5-2*	5'-GAATTCGCTTTAGCGCGGGCTTACCTCC-3'	
5-3*	5'-GAATTCCTCGTGTGCGTTCGACGCG-3'	
5-4*	5'-GGATCCTCAGTCAAGTGCTCGAGCGG-3'	
6-2*	5'-GAATTCCTTCTTGGGCAGGAGCTGCGC-3'	
6-3*	5'-GAATTCACGGGCCAGGCTGTTCTTACG-3'	
6-4	5'-GGATCCTTAATACTCTTGTGATTGAGAAGAACCCTTCTTTCC-3'	
p1	5'-AGTGTAGAATTATGTCGCGACGCGTA-3'	Plasmid construction for expression in <i>E. coli</i>
p2	5'-AAGTACAAGCTTCTACGTCAACGCGAC-3'	

*Primers 1-1 and 1-2 are used for amplifying *h2af1o*; 2-1 and 2-2 for *h2afx*; 3-1 and 1-2 for *h2af1o*(^dN), which directly combined with GFP; 1-1 and 4-2 for *h2af1o*(^dC), which directly combined with GFP; 2-1 and 5-2 for *h2afx*-N; 5-3 and 5-4 for *h2af1o*(^dN) for recombining with *h2afx*-N; 1-1 and 6-2 for *h2af1o*(^dC) for recombining with *h2afx*-C; 6-3 and 6-4 for *h2afx*-C.

MATERIALS AND METHODS

Fish Specimens

All procedures described herein were reviewed and approved by the Animal Care and Use Committee of the Institute of Hydrobiology, Chinese Academy of Sciences, and were performed in accord with the Guiding Principles for the Care and Use of Laboratory Animals. Gibel carp (*C. auratus gibelio*) and color crucian carp (*Carassius auratus*) were maintained at the Guanjiao Experimental Station of Institute of Hydrobiology, Wuhan, China. Induced spawning, artificial insemination, and embryo incubation were performed as described previously [28]. Zebrafish (*Danio rerio*) were maintained and spawned as described previously [34].

Sequence Analysis

Oocyte *h2af1o* cDNA was obtained from a cDNA library of fully grown oocytes of gibel carp [14]. Ubiquitous *h2afx* cDNA was obtained from large-scale sequencing of the previously set SMART (switch mechanism at the 5' end of RNA templates) cDNA library of gibel carp gastrula embryos [35].

Sequence alignments were performed using ClustalW1.8 (<http://www.ebi.ac.uk/Tools/clustalw2/index.html>) [36]. The shading of multiple alignment was performed using BOXSHADE 3.21 (http://www.ch.embnet.org/software/BOX_form.html), and identities were calculated using DNAMAN 6.0 (<http://en.bio-soft.net/format/DNAMAN.html>).

RT-PCR Analysis

Temporal expression was analyzed by RT-PCR in a volume of 25 μ l containing 1 ng cDNA and a pair of *h2af1o* cDNA-specific primers (Table 1). The PCR condition was 30 cycles at 94°C for 30 sec, 62°C for 30 sec, and 72°C for 40 sec. As a control, *bactin* was amplified from the same set of cDNA samples. All primers are listed in Table 1. The PCR products were separated on 1.5% agarose gel and documented using a bioimaging system (Syngene Division of SynGene Ltd.).

Riboprobe Synthesis and In Situ Hybridization

A 270-base pair (bp) cDNA fragment (Fig. 1A) amplified by primers *h2af1o*-1 and *h2af1o*-2 was cloned to pGEM-T vector (Promega) and linearized by *NotI* and *NcoI*, respectively. Antisense or sense digoxigenin-uridine triphosphate-labeled RNA probes were synthesized using T7 or Sp6 polymerase by in vitro transcription (DIG RNA labeling kit; Roche Molecular Biochemicals). In situ hybridization was performed according to the protocol previously published [35].

Histone Sample Preparation and Alkaline Phosphatase Treatment

Histone sample preparation from cells in transient expression followed the method reported by Pilch et al. [37], whereas histone samples from oocytes, tissues, and embryos were prepared with some improvements. The protocol was as follows. First, 200 oocytes or embryos, or about 10 mm³ of tissues, were homogenized in a 1.5-ml tube containing about 0.4 ml homogenization buffer (10 mM Tris-HCl [pH 7.5], 1 mM MgCl₂), and 25 μ l 10% NP-40 was added until there were no visible clumps in suspensions. After that, suspensions were homogenized more slowly to prevent foaming. Then, the suspensions were centrifuged at 16000 \times g for 1 min, and the supernatants were aspirated or drained off carefully and completely. Second, 1 ml salt wash buffer (10 mM Tris-HCl [pH 7.5], 1 mM MgCl₂, 0.4 M NaCl) was added to loosen the pellets; the mixture was incubated on ice for 15 min and then centrifuged at 16000 \times g for 1 min. After that, the supernatants were again aspirated or drained off carefully and completely. Third, 5 volumes of extraction solution (120 μ l concentrated H₂SO₄, 2 ml glycerol, 0.1 g 2-mercaptoethanolamine; add water to 10 ml) were added to the pellets, and the mixture was incubated at 4°C overnight. Fourth, the precipitates were pelleted at 16000 \times g for 10 min, and the supernatants containing histones were precipitated by trichloroacetic acid (TCA) (Sigma-Aldrich). Finally, the dried TCA precipitates were dissolved in SDS sample buffer (if the buffer turned yellow, NH₄OH was added to maintain the neutral pH, as indicated by the buffer turning blue) and placed in a water bath at 95°C for 5 min. The 15% resolving gel was used to separate histones in electrophoresis.

The protocol of alkaline phosphatase treatment for histones was described previously [38]. The pellets, collected after homogenizing (with homogenization buffer) and washing (with salt wash buffer) in histone sample preparation, were incubated with 20 U calf intestinal phosphatase (p4252; Sigma-Aldrich) and diluted in alkaline phosphatase buffer (100 mM NaCl, 5 mM MgCl₂, 100 mM Tris [pH 9.5]) at 37°C overnight [39]. Afterward, the mixture was centrifuged at 16000 \times g for 1 min, and the supernatant was discarded. Then, the histones were extracted from pellets with extraction solution. For transfected cells, we also prepared histone extracts, lytic cell supernatants, and salt wash supernatants according to the protocols described by Pilch et al. [37].

Antiserum Preparation and Western Blot Detection

A partial cDNA fragment encoding a 23-amino acid-specific peptide of the N-terminal of H2af1o (MSGRGKKLVAAAPKSKSSSVSRST), whose main part is different from that of other histone H2As (Fig. 1B), was fused in frame to the His-tag by insertion between the *EcoRI* and *HindIII* sites in pET-32 α (+) (Novagen). The recombinant fusion protein was expressed in *Escherichia coli* (BL21 [DE3] pLysS) and purified using the RoboPop Ni-NTA HisBind

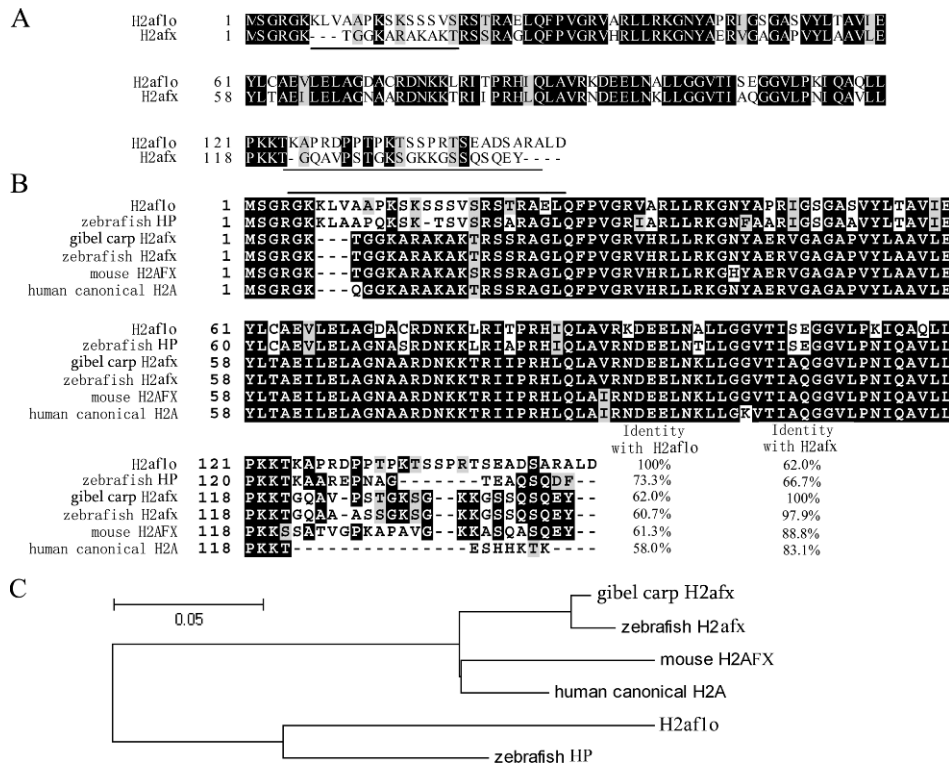


FIG. 1. Sequence alignments and phylogenetic analysis of H2af1o and H2afx. **A)** Alignment of the protein sequences of H2af1o and H2afx. The underlined regions indicate the main sequence differences between H2af1o and H2afx at the N-terminal and C-terminal. **B)** Multiple alignments of H2af1o and H2afx with related histone H2As; identical regions are shaded, and suspension points represent the omitted amino acids. The identities of H2af1o (or H2afx) compared with other histone H2As are listed. **C)** Phylogenetic tree of H2af1o, H2afx, and related H2As. The accession numbers of these sequences are as follows: H2af1o (AF315728), zebrafish hypothetical protein (zebrafish HP) (XP_699392), gibel carp H2afx (EU734830), zebrafish H2afx (NP_957367), human canonical H2A (CAB06031), and mouse H2AFX (P27661). The phylogenetic tree was generated using neighbor-joining analysis. Bar represents 5% estimated phylogenetic divergence.

purification kit according to the manufacturer's protocol (Novagen). For preparation of a polyclonal antibody against H2af1o, the purified protein (500 µg) was emulsified in complete Freund adjuvant (Sigma-Aldrich) and injected into the rabbit lymph. After 2 wk, the rabbit was subcutaneously booster immunized once with the same amount of protein emulsified in incomplete Freund adjuvant (a total of two injections). Ten days later, antiserum was collected and stored in aliquots at -20°C . Antibody specificity was demonstrated by Western blot using the expressing recombinant protein and the histone sample of eggs. Western blot detection followed the protocol previously published [27, 39, 40]. All chemicals were purchased from Sigma-Aldrich.

Construction of GFP Fusion Constructs

The *GFP-h2af1o* and *GFP-h2afx* constructs were generated by inserting the corresponding cDNAs into pEGFP-C1 vector (Invitrogen). First, the cDNA fragments were inserted into pGEM-T vector between the *Bgl*III and *Eco*RI sites. Then, they were respectively introduced to pEGFP-C1 vector between the same sites. Based on three domains of histone H2A [41, 42], H2af1o was divided into N-terminal tail (1–17 amino acids), globular domain (18–123 amino acids), and C-terminal tail (124–150 amino acids), and H2afx was divided into N-terminal tail (1–15 amino acids), globular domain (16–120 amino acids), and C-terminal tail (121–142 amino acids).

To generate the *GFP-h2af1o*(^ΔN) and *GFP-h2af1o*(^ΔC) constructs, the corresponding cDNA was amplified with the *Bgl*III and *Eco*RI sites using *GFP-h2af1o* as template. The 18- to 150-amino acid coding sequence of H2af1o for constructing *GFP-h2af1o*(^ΔN), as well as the 1- to 123-amino acid coding sequence for constructing *GFP-h2af1o*(^ΔC), was amplified correspondingly. The PCR fragments were introduced into pEGFP-C1 vector using the same method as that for the *GFP-h2af1o* construct.

To generate the *GFP-h2af1o*(h2afx-N) construct, *h2af1o*(^ΔN) with the *Eco*RI and *Bam*HI sites was also amplified from *GFP-h2af1o*, and *h2afx*-N with the *Bgl*III and *Eco*RI sites was amplified from the 1- to 15-amino acid coding sequence of H2afx using *GFP-h2afx* as template. First, *h2af1o*(^ΔN) to pEGFP-C1 vector was inserted between the *Eco*RI and *Bam*HI sites, and then *h2afx*-N was introduced to the *Bgl*III and *Eco*RI linearized plasmid.

To generate the *GFP-h2af1o*(h2afx-C) construct, *h2af1o*(^ΔC) with the *Bgl*III and *Eco*RI sites was also amplified from *GFP-h2af1o*, and *h2afx*-C with the *Eco*RI and *Bam*HI sites was amplified from the 121- to 142-amino acid coding sequence of H2afx using *GFP-h2afx* as template. Also, *h2af1o*(^ΔC) to pEGFP-C1 vector was inserted between the *Bgl*III and *Eco*RI sites first, and then the *h2afx*-C was introduced to the *Eco*RI and *Bam*HI linearized plasmid.

Primers were used in constructing the vectors. These are listed in Table 1.

Living Cell Microscopy and FRAP Analysis

Carassius auratus blastulae embryonic cells were maintained as previously described [43, 44]. Cells were transfected with the constructs using Lipofectamine (Invitrogen) according to the manufacturer's protocol. Images of living cells and time-series FRAP images were obtained using an Olympus FV1000 confocal microscope equipped with a 181 60 × 1.3 N.A. oil immersion objective and an argon laser of 488-nm wavelength.

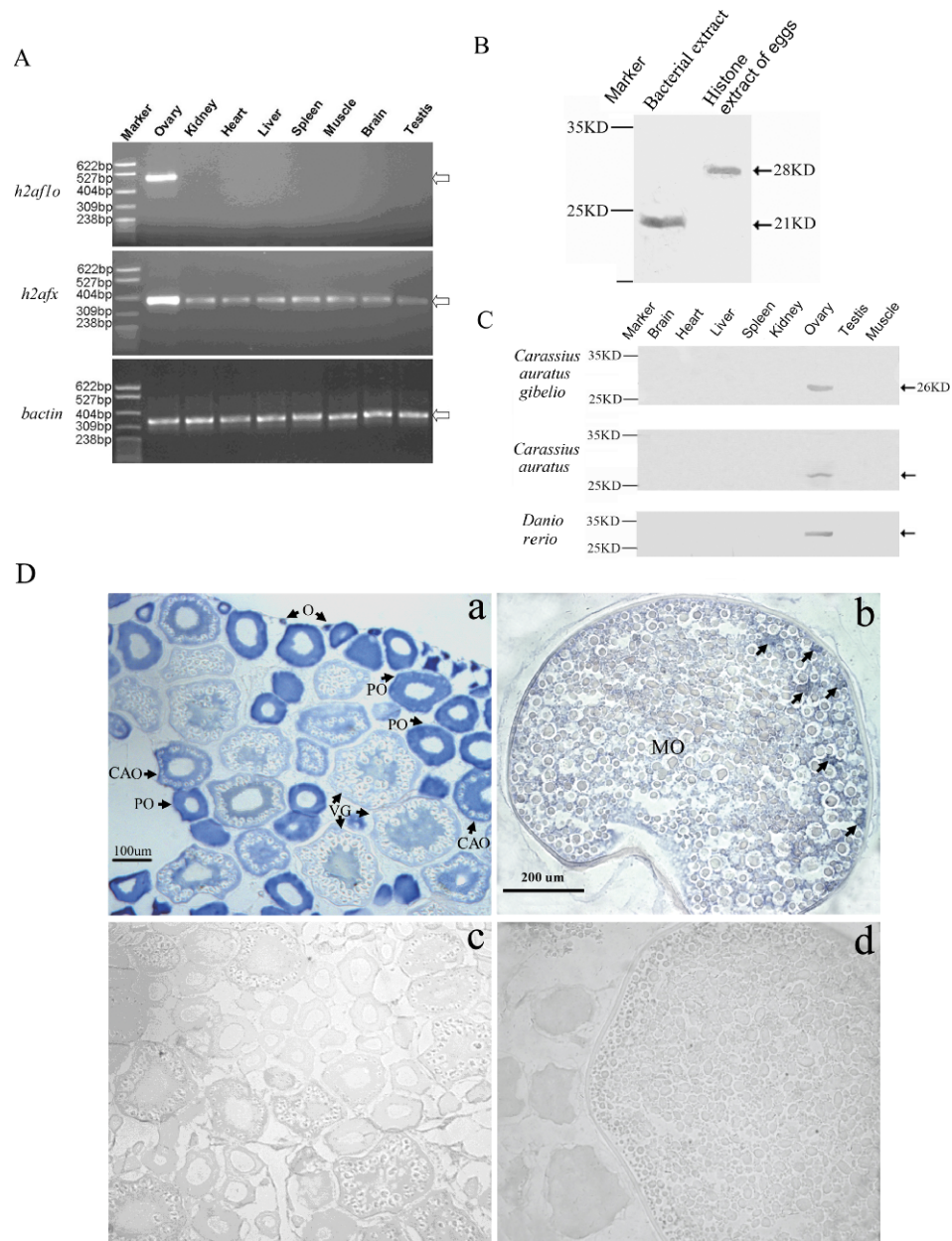
For each FRAP experiment, a small nuclear area ($2 \times 2 \mu\text{m}^2$) was photobleached in a single cell, and images were collected at concurrent intervals. FRAP image data analysis was conducted according to the protocol previously described [45, 46]. Statistical analyses of these experiments were performed using Microsoft Excel and SPSS 13.0. For each construct, the mean (SD) of five parallel data sets was calculated, and the significance ($P < 0.05$) of recovery curves between two corresponding constructs was compared using repeated-measures ANOVA and post hoc tests of least significant difference.

RESULTS

Molecular Characterization and Primary Structure Difference of Core Histone H2a Variant and Ubiquitous h2afx in Gibel Carp

To characterize the core histone H2a variant and to reveal its primary structure difference, we first cloned the full-length cDNA of ubiquitous *h2a* from the gastrula SMART cDNA library of *C. auratus gibelio* [35, 47]. Comparing ubiquitous *h2a* and the *h2a* variant from oocytes, we found significant differences in their sequences. The histone *h2a* variant full-length cDNA is 587 bp, containing an open reading frame (ORF) of 453 bp encoding a peptide of 150 amino acids, and has a 87-bp 5' untranslated region (UTR) and a 47-bp 3' UTR [14]. However, ubiquitous *h2a* full-length cDNA is 676 bp, containing an ORF of 429 bp encoding a peptide of 142 amino acids, and has a 55-bp 5' UTR and a 192-bp 3' UTR. Because of many nucleotide mutations in the histone *h2a* variant, especially deletion and addition in the sequences encoding its N-terminal and C-terminal, the stop codon (TGA) is slipped 29 bp downstream; therefore, the ORF is longer than that of ubiquitous *h2a*. Consequently, the amino acid identity of the

FIG. 2. Ovary-specific expression of *h2af1o*. **A**) The RT-PCR analysis of *h2af1o* and *h2afx* transcripts (arrow) in various tissues, with *bactin* as control (arrow). **B**) The specificity of the polyclonal antibody of H2af1o proved by Western blot analysis. **C**) Western blot detection of H2af1o in various tissues of *C. auratus gibelio*, *C. auratus*, and *D. rerio*. **D**) *h2af1o* RNA localization during oogenesis. Ovarian cross sections after in situ hybridization with antisense (**a** and **b**) or sense (**c** and **d**) *h2af1o* probe. CAO, cortical alveolus-stage oocyte; KD, kilodaltons; MO, maturing oocyte; O, oogonia; PO, primary growth-stage oocyte; VG, vitellogenic oocyte. Arrows in **b** indicate the *h2af1o* transcript signal. Bars = 100 μ m (**a**, **c**) and 200 μ m (**b**, **d**).



two deduced proteins is only 62%, and primary differences exist in the N-terminal and C-terminal. As shown in Figure 1A, there are three extra and 10 various amino acids in the histone H2a variant N-terminal, and five serines (the possible phosphorylated sites) are added into the various residues. More significant differences exist in the C-terminal. Compared with the relative sequence of ubiquitous H2a, 22 different residues exist in the H2a variant C-terminal, in which there also are five extra residues.

To clarify the two H2a subtypes, we performed amino acid alignment and phylogenetic tree analysis. As shown in Figure 1B, the H2a variant is closest to a zebrafish hypothetical protein, with 73.3% identity, whereas the identities to zebrafish H2afx, mouse H2AFX, and human canonical H2A are only 60.7%, 61.3%, and 58.0%, respectively. Significantly, ubiquitous H2a has 97.9%, 88.8%, and 83.1% identities to zebrafish H2afx, mouse H2AFX, and human canonical H2A, respectively, and only 66.7% identity to zebrafish hypothetical protein. In addition, ubiquitous H2a contains the Ser-Gln motif that is the sequence mark for H2afx [5, 48] in its C-terminal

sequence, whereas there is no Ser-Gln motif in the H2a variant. Phylogenetic tree construction indicates that ubiquitous H2a is clustered with zebrafish H2afx, mouse H2AFX, and human canonical H2A, whereas the H2a variant and zebrafish hypothetical protein are clustered together (Fig. 1C). Therefore, these data suggest that ubiquitous H2a is an H2afx homologue in *C. auratus gibelio* and that the H2a variant is a novel H2a variant. Moreover, H2AFX is closest to canonical H2A not only in sequence but also in function [32, 48, 49]; therefore, we used gibel carp H2afx as a ubiquitous H2A control in this study.

Oocyte-Specific Expression Pattern and Phosphorylation Modification of H2af1o During Oocyte Maturation

The RT-PCR in adult tissues indicated that the *h2a* variant was transcribed only in ovary, whereas gibel carp *h2afx* was ubiquitously transcribed in all examined tissues, including ovary, brain, liver, spleen, kidney, muscle, heart, and testis (Fig. 2A). To further confirm the ovary-specific expression, we

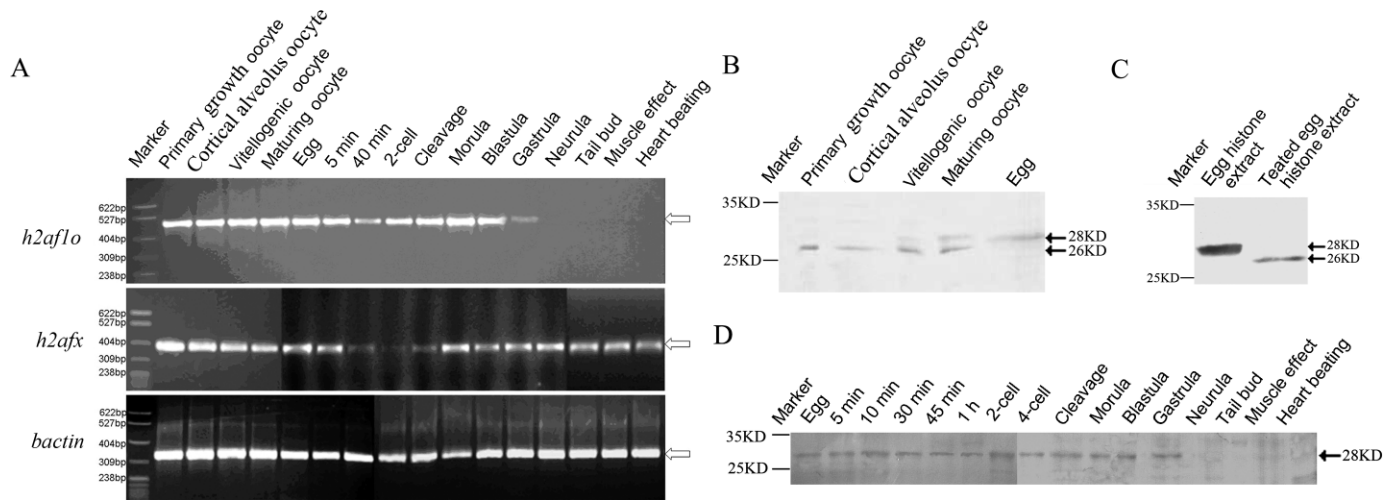


FIG. 3. Expression pattern of *h2af1o* during oogenesis and early embryogenesis. **A**) The RT-PCR analysis of *h2af1o* and *h2afx* transcripts (arrow) during oogenesis and embryogenesis, with *bactin* as control (arrow). **B**) Western blot detection of H2af1o during oocyte maturation. **C**) Western blot detection of H2af1o before and after alkaline phosphatase treatment in mature eggs. **D**) Western blot detection of H2af1o during embryogenesis. KD, kilodaltons.

prepared a polyclonal antibody using a His-tag recombinant protein containing the N-terminal 23 amino acids of the H2a variant (MSGRGKKLVAAAPKSKSSSVSRST). The antibody recognized a 21-kDa His-tag recombinant peptide in bacterial extract and a natural 28-kDa protein in histone extract of mature eggs (Fig. 2B). Using the polyclonal antibody for Western blot analysis, we then detected a specific protein band at about 26 kDa in ovary but not in other tissues (Fig. 2C). Furthermore, we used the antibody in two other bisexual fish species, color crucian carp (*C. auratus*) and zebrafish (*D. rerio*). Intriguingly, a similar protein band was detected only in ovary of the two fish species (Fig. 2C). These data suggest that fish oocytes contain the H2a variant.

To reveal cell types of the H2a variant expression in ovary, we performed in situ hybridization of ovary tissue by using an N-terminal 270-bp cDNA fragment of the *h2a* variant (Fig. 1A) as probe. As shown in Figure 2D, according to the dividing stage criteria in zebrafish [50], strong signal can be observed in oogonia and in oocytes of different developmental stages (such as primary growth-stage oocytes, cortical alveolus-stage oocytes, vitellogenic oocytes, and maturing oocytes). In oogonia and primary growth-stage oocytes, the *h2a* variant transcript signal is uniformly distributed in the cytoplasm. From cortical alveolus-stage oocytes to maturing oocytes, the transcript signal is mainly concentrated in peripheral cytoplasm. Especially in primary growth-stage oocytes and cortical alveolus-stage oocytes, the concentrated speckles are easily observed in the peripheral cytoplasm. Significantly, no positive signal is seen in somatic cells surrounding oocytes. These data confirm that the *h2a* variant is specifically expressed not only in ovary but also in oocytes throughout oogenesis. Therefore, it is a novel oocyte-specific *h2a* variant, designated as *h2af1o* (H2A histone family, member 1, oocyte specific).

Moreover, we detected the *h2af1o* transcript by RT-PCR in oocytes and embryos at different developmental stages during oogenesis and embryogenesis. As shown in Figure 3A, the *h2af1o* transcript is abundant in oocytes of all developmental stages and in embryos from fertilization to early gastrulation and declines dramatically in gastrula embryos, and no transcript is detected in other embryos after gastrulation. The gibel carp *h2afx* transcript exists throughout oogenesis and embryogenesis. The maternal transcript decreases after fertilization, but the zygote *h2afx* reappears in the embryos after the

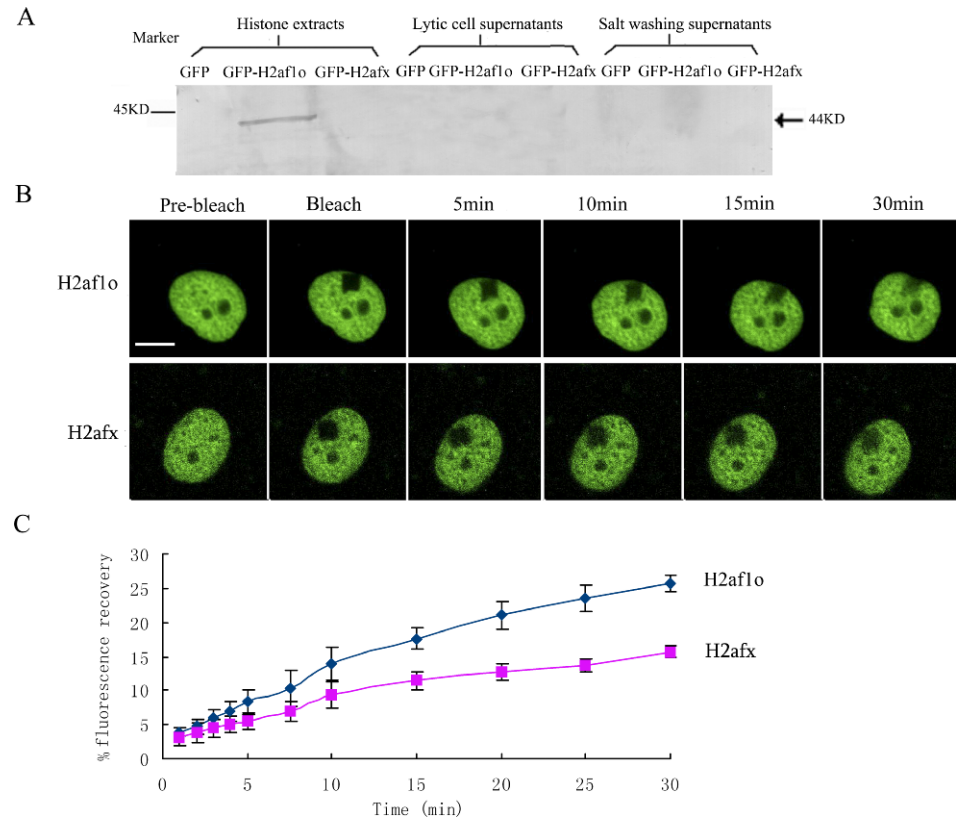
morula stage. Western blot detection revealed significant modification of H2af1o during oogenesis and oocyte maturation. As shown in Figure 3B, only one H2af1o protein band at about 26 kDa is detected in primary growth oocytes and cortical alveolus oocytes. When the oocytes develop to vitellogenesis and maturation stages, another 28-kDa protein band is detected, and the content increases with oocyte maturation. Subsequently, only the 28-kDa protein band is observed in mature eggs, whereas the 26-kDa protein band disappears. This suggests that posttranslational modification of H2af1o may result in a mobility shift during oocyte maturation. We performed alkaline phosphatase treatment because many possible phosphorylation sites were predicted in the H2af1o sequence. Figure 3C shows the results detected by Western blot. When the egg histone extract was treated with calf intestine alkaline phosphatase, the 28-kDa H2af1o protein band in the egg histone extract became 26 kDa, which is similar to the size in primary growth oocytes and cortical alveolus oocytes. The mobility shift indicates that H2af1o phosphorylation occurs during oocyte maturation.

We also detected the existence of H2af1o protein in embryos of different stages by Western blot. Similar to the *h2af1o* transcript, it was detected only in early embryos before gastrulation, and no H2af1o protein was found in other embryos after gastrulation (Fig. 3D). This further confirms that H2af1o is specifically expressed in oocytes and exists only in early embryos.

H2af1o Has Higher Mobility than Ubiquitous H2afx in Living Cell Nuclei

Dynamic binding of histones in nucleosomes has been confirmed [7, 33], and a histone variant with specified molecular and expressional characteristics represents specialized mobility [12, 51], which reflects DNA-binding affinity and nucleosome stability [6]. To understand binding dynamics of the novel core histone variant H2af1o in nucleosomes and to reveal differences between H2af1o and ubiquitous H2afx, we further investigated the dynamic exchange of GFP-tagged H2af1o and GFP-tagged H2afx in chromatin by FRAP, which can be used to define the mobility of molecules in living cell nuclei [51]. Moreover, ubiquitous H2afx was used as a conventional histone control for H2af1o, as H2AFX displayed

FIG. 4. Dynamic exchange of H2af1o and H2afx. **A)** Western blot detection of GFP-H2af1o recombinant protein in histone extracts, lytic cell supernatants, and salt wash supernatants from the cells expressing GFP, GFP-H2af1o, and GFP-H2afx. KD, kilodaltons. **B)** The nuclei of cells expressing either H2af1o or H2afx were imaged before and after photobleaching of chromatin foci at the indicated time points. Bar = 5 μ m. **C)** Quantitative fluorescence recovery curves of H2af1o and H2afx. The recovery of the fluorescent signal was monitored by time-lapse microscopy and was measured using ImageJ (<http://rsb.info.nih.gov/ij/index.html>). Values represent the mean \pm SD for five nuclei from three independent experiments.



mobility similar to that of canonical histone H2A in a FRAP experiment [32].

To confirm GFP-H2af1o expression and its association with chromatin, three types of extracts (histone extracts, lytic cell supernatants, and salt wash supernatants) were prepared from transfected cells with only *GFP* plasmid, the *GFP-h2af1o* construct, and the *GFP-h2afx* construct, respectively, and were subjected to Western blot detection using anti-H2af1o antibody. As shown in Figure 4A, only a fusion GFP-H2af1o protein band is detected in histone extract from transfected cells with the *GFP-h2af1o* construct, whereas no positive band was detected in histone extracts from transfected cells with *GFP-h2afx* construct or with only *GFP* plasmid. Significantly, the expressed fusion GFP-H2af1o protein exists only in histone extract, whereas there is no fusion GFP-H2af1o protein in free and soluble proteins of the lytic cell supernatants and weakly binding proteins in the salt wash supernatants. These data indicate that the expressed fusion GFP-H2af1o protein is associated with chromatin and is incorporated into nucleosomes.

Moreover, wild-type GFP green signal was ubiquitously distributed in the nucleus and in the cytoplasm (data not shown), whereas the green signal of GFP-H2af1o or GFP-H2afx strictly localizes in the nucleus (Fig. 4B, pre-bleach). FRAP analysis not only revealed gradual recovery in the bleached regions of nuclei after photobleaching but also revealed a significant recovery difference between GFP-H2af1o and GFP-H2afx (Fig. 4B). As shown in Figure 4C, only 15.7% of the GFP-H2afx initial value is recovered 30 min after photobleaching, whereas 25.6% of the GFP-H2af1o initial value is recovered. The faster recovery and the significant recovery difference between GFP-H2af1o and GFP-H2afx ($F = 60.28$, $P < 0.001$) suggest that H2af1o has higher mobility than ubiquitous H2afx in the transfected nuclei.

H2af1o Has a More Protruding N-Terminal and a Tightly Binding C-Terminal

Deletion mutants, *GFP-h2af1o*(ΔN) and *GFP-h2af1o*(ΔC), were constructed (Fig. 5A) based on the specific sequence in the N-terminal and C-terminal of H2af1o (Fig. 1B) and were analyzed by FRAP to test whether the specific tails have any specific binding ability. Loss of the C-terminal domain fundamentally changed its cellular location; therefore, the expressed protein signal existed not only in the nucleus but also in the cytoplasm (Fig. 5B). FRAP results showed that H2af1o(ΔC) cannot be bleached completely under the same conditions set for H2af1o and exhibits a very quick recovery within 18 sec (Fig. 5B). This indicates that H2af1o(ΔC) has rapid and nonconstrained motion and that it does not bind or very weakly binds to chromatin. Therefore, the C-terminal domain of H2af1o is responsible for correct nuclear distribution. However, H2af1o without an N-terminal tail still exhibits a nuclear location (Fig. 5C). Moreover, the FRAP recovery rate of GFP-H2af1o(ΔN) is higher than that of GFP-H2af1o ($F = 10.03$, $P < 0.001$), and about 59.1% of its initial value is recovered 30 min after bleaching (Fig. 5D). These observations reflect weak binding affinity of the N-terminal of H2af1o and very tight binding of its C-terminal. Therefore, H2af1o is a histone variant with a protruding N-terminal and a tightly contracting C-terminal, different from canonical histone H2A, whose C-terminal protrudes from nucleosome core particles [52].

To review the detailed binding difference of N-terminal and C-terminal tails between H2af1o and ubiquitous H2afx, the chimeric proteins GFP-H2af1o(H2afx-N) and GFP-H2af1o(H2afx-C) were expressed and subjected to FRAP analysis. As shown in Figure 5C, both chimeric proteins exhibit typical histone distribution in the nucleus. Substituting the N-terminal of H2af1o with that of H2afx results in the slowest recovery, in

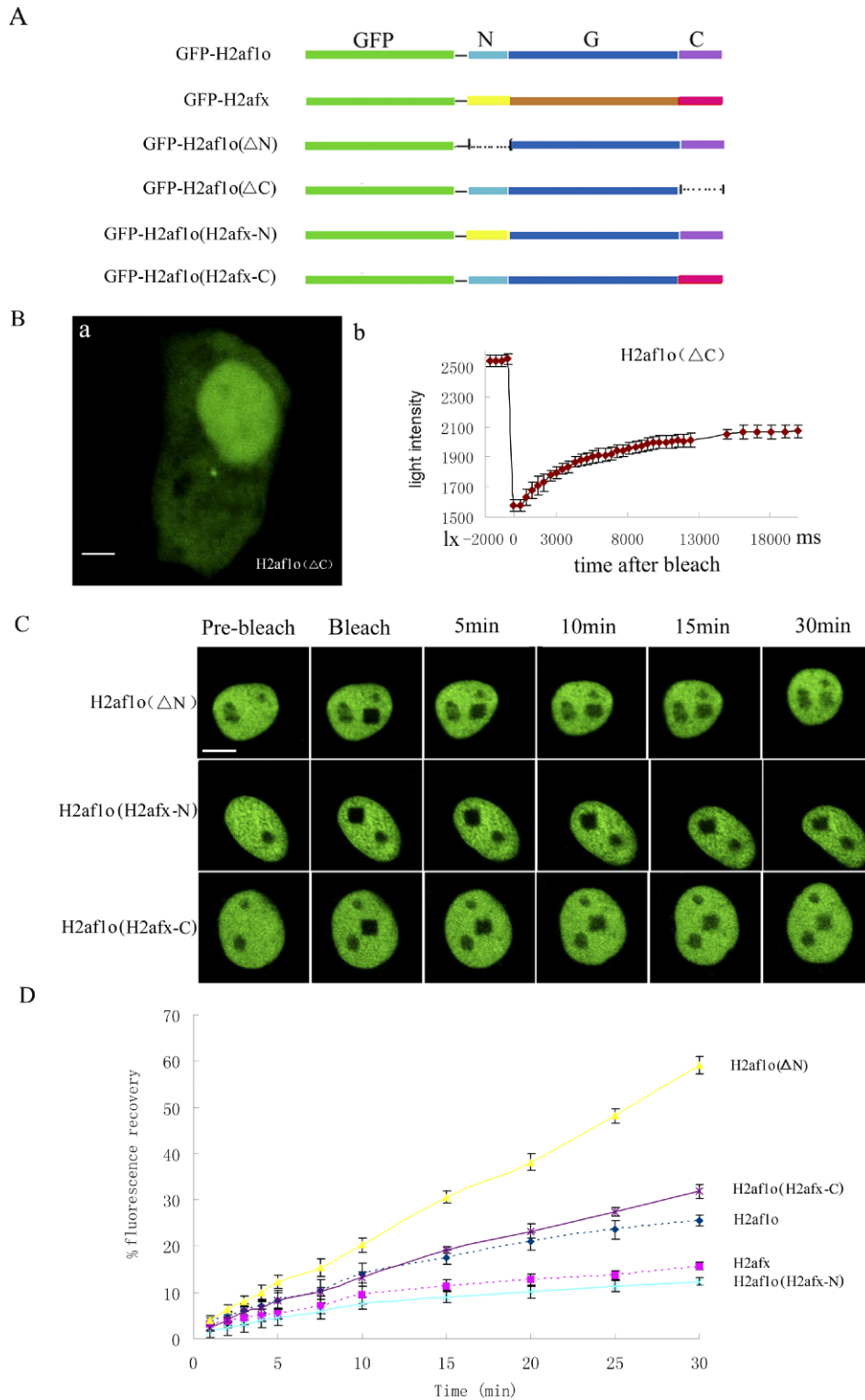


FIG. 5. Dynamic exchange in H2af1o deletion mutants and isoform chimeras. **A)** Schematic representation of GFP-labeled H2af1o, H2afx, deletion mutants, and isoform chimeras. C, C-terminal domain; G, globular domain; N, N-terminal domain. **B)** Dynamic exchange of H2af1o(Δ C). The photograph shows its nonconstrained cellular distribution (**a**), along with its quantitative fluorescence recovery curves in milliseconds (ms) (**b**). The recovery of the fluorescent signal was monitored using time-lapse microscopy and was measured by the Olympus FV1000 software automatically. Values represent the mean \pm SD for five nuclei from three independent experiments. Bar = 5 μ m. **C)** The nuclei of cells expressing H2af1o(Δ N), H2af1o(H2afx-N), or H2af1o(H2afx-C) were imaged before and after photobleaching of chromatin foci at the indicated time points. Bar = 5 μ m. **D)** Quantitative fluorescence recovery curves of H2af1o(Δ N), H2af1o(H2afx-N), and H2af1o(H2afx-C), with curves of H2af1o and H2afx indicated by the dotted lines for comparison. The recovery of the fluorescent signal was monitored by time-lapse microscopy and was measured using ImageJ. Values represent the mean \pm SD for five nuclei from three independent experiments.

which only 12.4% of its initial value is recovered 30 min after bleaching. Compared with H2af1o, H2afx, H2af1o(Δ N), and H2af1o(H2afx-C), the recovery curves are $P < 0.001$, $P = 0.005$, $P < 0.001$, and $P < 0.001$, respectively (Fig. 5D). This indicates higher binding affinity of the N-terminal of H2afx compared with that of H2af1o; in other words, the N-terminal of H2af1o can release from nucleosomes more easily. However, substituting the C-terminal of H2af1o with that of H2afx increases the recovery of H2af1o, with the recovery rate rising to 31.8% of its initial value 30 min after bleaching.

Compared with the original H2af1o, the difference is not significant before 10 min ($F = 0.34$, $P = 0.58$), but a significant difference can be observed from 10 min to 30 min after bleaching ($F = 27.72$, $P < 0.001$) (Fig. 5D). The phenomenon indicates that the binding affinity of the C-terminal of H2afx is weaker than that of H2af1o and confirms tight binding of the C-terminal of H2af1o as revealed by the deletion mutant. Overall, our data demonstrate that H2af1o compared with ubiquitous H2afx has a tightly binding C-terminal and a more weakly binding N-terminal.

DISCUSSION

Oocyte maturation and fertilization are characterized by dramatic global chromatin remodeling events, including global changes in histone modification and histone exchange [31]. Histones have dual functions in the nucleus as important structural components and as regulators of gene expression. Herein, we identified and characterized the novel oocyte-specific histone variant *h2af1o* in fish. As its control, we also identified ubiquitous *h2afx*, which has molecular characteristics and expression patterns that are typical of somatic histone H2A. We found significant differences in expression patterns and nucleosome dynamics between them. In contrast to ubiquitous expression of *h2afx*, expression of *h2af1o* occurs only in oocytes in a gametogenic stage-specific manner and can persist until early gastrulation in embryos. Also, H2af1o is hyperphosphorylated during oocyte maturation. Moreover, H2af1o confers higher mobility in nucleosomes compared with ubiquitous H2afx, and it has a more flexible N-terminal and a more tightly binding C-terminal.

Another intriguing finding of this study is posttranslational modification of H2af1o. Binding of histone variants to the chromatin template and posttranslational modification at the histone tails contribute to the establishment of epigenetic modification in the oocyte genome [5, 53]. Histone modification can distinguish euchromatin from heterochromatin, and it influences associations of proteins and protein complexes that regulate gene transcription or repression by altering the availability of genes to transcription factors [54]. Our data prove that H2af1o is hyperphosphorylated during oocyte maturation. To date, the most studied phosphorylation of histone H2A is S1 phosphorylation in mitotic chromatin. It was reported to inhibit transcription on chromatin templates [55]. Evolutionarily conserved phosphorylation of H2A during the cell cycle may have a dual purposes in chromatin condensation during mitosis and in histone deposition during the S phase [56]. Therefore, phosphorylation of H2af1o may be critical to mitotic chromatin during fast cleavage. In addition, the antibody against the N-terminal of H2af1o detected bands not of the estimated 17 kDa but similar to the size of those of monoubiquitinated H2A [57]. In preliminary experiments, we prepared another antibody against the C-terminal peptide of H2af1o; however, the antibody could not recognize H2af1o protein (data not shown). This may be because monoubiquitin always modifies the amino acid (lys 119) in the C-terminal tail of H2A [1, 57], which in turn modified the antigen of the C-terminal. Therefore, monoubiquitination likely takes place in the chromatin-binding H2af1o, as histone preparation can isolate histones incorporated into chromatin but not histones in the soluble core histone pool. Monoubiquitinated histone H2A was reported to be involved in transcriptional repression of the maternal genome [57, 58]. Therefore, phosphorylation and monoubiquitination of H2af1o may maintain transcriptional silence of the maternal genome during oogenesis and early embryogenesis.

The FRAP recovery rates of GFP-labeled H2af1o, H2afx, and their mutants provide additional information about the dynamics of nucleosomes incorporated with each protein and about the specific binding affinity of the N-terminal and C-terminal of H2af1o. H2af1o is less tightly bound compared with H2afx in the nucleosome core particle, suggesting lower inherent stability of H2af1o to the conventional H2A. In this regard, the nucleosome containing H2af1o may be more relaxed. Its C-terminal domain tightly binds to nucleosome core particles, whereas its N-terminal domain releases to a large degree. Considering the fast replication of chromosomes from

early embryonic cleavage up to blastocyte stage or early gastrulation, special binding of domains in H2af1o may provide more potential covalent modification sites in its protruded N-terminal to receive abundant downstream signals, while keeping the nucleosomes in a stable state via its tightly bound C-terminal along with the remaining globular domain.

Our results suggest that H2af1o may have intrinsic ability to modify chromatin properties. Incorporation of the histone H2A variant, modification of its tails, and binding of chromatin-associated proteins cause nucleosome remodeling [59], which has an important role in regulating temporal and spatial gene activation in oocyte maturation and early embryonic cleavage [60]. Therefore, H2af1o is probably involved in the resetting of gametic epigenetic patterns necessary to repress transcription during early cleavage, when somatic histone H2a is absent or insufficiently abundant. The less stable H2af1o-bearing nucleosomes can also provide more surfaces for adding epigenetic information needed for downstream signaling. A future challenge is to identify the specific chaperone for H2af1o, as histone variants have chaperones different from those of canonical histones [5, 61]. The existence of a similar oocyte-specific H2a variant in color crucian carp and zebrafish suggests that the novel oocyte-specific H2a variant may be an essential factor for regulating development in oocytes and early embryos.

In summary, H2af1o is an oocyte variant of H2a and has a unique role in oocyte development because of its differential phosphorylation. Core histones are usually highly conserved proteins, and linker histone has more than one form within species and is less conserved than core histones. To date, the oocyte-specific variant has been limited to the H1 linker histone. In this regard, identification of the gibel carp oocyte-specific H2a variant represents a novel finding. In our study, we identified an oocyte-specific core histone H2A variant in fish and demonstrated its expression pattern and high mobility, but more research is needed to better understand its physiological function and acting mechanisms in oocyte development and early embryogenesis.

ACKNOWLEDGMENTS

We thank professors Qing-Ming Luo and Shao-Qun Zeng and associate professor Zhi-Hong Zhang for allowing and helping us to use the Olympus FV1000 confocal microscope.

REFERENCES

1. Cosgrove MS. Histone proteomics and the epigenetic regulation of nucleosome mobility. *Expert Rev Proteomics* 2007; 4:465–478.
2. Wu N, Gui JF. Histone variants and histone exchange [in Chinese]. *Yi Chuan* 2006; 28:493–500.
3. Guillemette B, Gaudreau L. Reuniting the contrasting functions of H2A.Z. *Biochem Cell Biol* 2006; 84:528–535.
4. Ramaswamy A, Ioshikhes I. Global dynamics of newly constructed oligonucleosomes of conventional and variant H2A.Z histone. *BMC Struct Biol* 2007; 7:e76.
5. Bernstein E, Hake SB. The nucleosome: a little variation goes a long way. *Biochem Cell Biol* 2006; 84:505–517.
6. Henikoff S, Furuyama T, Ahmad K. Histone variants, nucleosome assembly and epigenetic inheritance. *Trends Genet* 2004; 20:320–326.
7. Jin J, Cai Y, Li B, Conaway RC, Workman JL, Conaway JW, Kusch T. In and out: histone variant exchange in chromatin. *Trends Biochem Sci* 2005; 30:680–687.
8. Eirin-Lopez JM, Ishibashi T, Ausio J. H2A.Bbd: a quickly evolving hypervariable mammalian histone that destabilizes nucleosomes in an acetylation-independent way. *FASEB J* 2008; 22:316–326.
9. Bassing CH, Suh H, Ferguson DO, Chua KF, Manis J, Eckersdorff M, Gleason M, Bronson R, Lee C, Alt FW. Histone H2AX: a dosage-dependent suppressor of oncogenic translocations and tumors. *Cell* 2003; 114:359–370.

10. Costanzi C, Pehrson JR. Histone macroH2A1 is concentrated in the inactive X chromosome of female mammals. *Nature* 1998; 393:599–601.
11. Changolkar LN, Singh G, Pehrson JR. macroH2A1-dependent silencing of endogenous murine leukemia viruses. *Mol Cell Biol* 2008; 28:2059–2065.
12. Gautier T, Abbott DW, Molla A, Verdel A, Ausio J, Dimitrov S. Histone variant H2ABbd confers lower stability to the nucleosome. *EMBO Rep* 2004; 5:715–720.
13. Gonzalez-Romero R, Mendez J, Ausio J, Eirin-Lopez JM. Quickly evolving histones, nucleosome stability and chromatin folding: all about histone H2A.Bbd. *Gene* 2008; 413:1–7.
14. Xie J, Wen JJ, Chen B, Gui JF. Differential gene expression in fully-grown oocytes between gynogenetic and gonochoristic crucian carps. *Gene* 2001; 271:109–116.
15. Dong CH, Yang ST, Yang ZA, Zhang L, Gui JF. A C-type lectin associated and translocated with cortical granules during oocyte maturation and egg fertilization in fish. *Dev Biol* 2004; 265:341–354.
16. Mei J, Chen B, Yue H, Gui JF. Identification of a C1q family member associated with cortical granules and follicular cell apoptosis in *Carassius auratus gibelio*. *Mol Cell Endocrinol* 2008; 289:67–76.
17. Furuya M, Tanaka M, Teranishi T, Matsumoto K, Hosoi Y, Saeki K, Ishimoto H, Minegishi K, Iritani A, Yoshimura Y. H1foo is indispensable for meiotic maturation of the mouse oocyte. *J Reprod Dev* 2007; 53:895–902.
18. Marzluff WF, Sakallah S, Kelkar H. The sea urchin histone gene complement. *Dev Biol* 2006; 300:308–320.
19. Song JL, Wessel GM. How to make an egg: transcriptional regulation in oocytes. *Differentiation* 2005; 73:1–17.
20. Gui JF. Genetic Basis and Artificial Control of Sexuality and Reproduction in Fish. Beijing: Science Press; 2007; 2007:107–124.
21. Jalabert B. Particularities of reproduction and oogenesis in teleost fish compared to mammals. *Reprod Nutr Dev* 2005; 45:261–279.
22. Chen B, Guo W, Gui JF. Expression characterization of ZP3 gene and isolation of chorion ZP3 protein in *Carassius auratus gibelio*. *Acta Hydrobiol Sinica* 2005; 29:233–238.
23. Fan LC, Yang ST, Gui JF. Differential screening and characterization analysis of the egg envelope glycoprotein ZP3 cDNAs between gynogenetic and gonochoristic crucian carp. *Cell Res* 2001; 11:17–27.
24. Wen J, Xie J, Gui J. cDNA cloning and characterization of a novel SNX gene differentially expressed in previtellogenic oocytes of gibel carp. *Comp Biochem Physiol B Biochem Mol Biol* 2003; 136:451–461.
25. Chen B, Gui J. Identification of a novel C1q family member in color crucian carp (*Carassius auratus*) ovary. *Comp Biochem Physiol B Biochem Mol Biol* 2004; 138:285–293.
26. Wang XL, Sun M, Mei J, Gui JF. Identification of a Spindlin homolog in gibel carp (*Carassius auratus gibelio*). *Comp Biochem Physiol B Biochem Mol Biol* 2005; 141:159–167.
27. Wang HY, Zhou L, Gui JF. Identification of a putative oocyte-specific small nuclear ribonucleoprotein polypeptide C in gibel carp. *Comp Biochem Physiol B Biochem Mol Biol* 2007; 146:47–52.
28. Gui JF, Liang SC, Zhu LF. Preliminary confirmation of gynogenetic reproductive mode in artificially multiple tetraploid allogynogenetic silver crucian carp. *Chin Sci Bull* 1993; 38:327–331.
29. Zhou L, Gui JF. Karyotypic diversity in polyploid gibel carp, *Carassius auratus gibelio* Bloch. *Genetica* 2002; 115:223–232.
30. Zhou L, Wang Y, Gui JF. Genetic evidence for gonochoristic reproduction in gynogenetic silver crucian carp (*Carassius auratus gibelio* Bloch) as revealed by RAPD assays. *J Mol Evol* 2000; 51:498–506.
31. Becker M, Becker A, Miyara F, Han Z, Kihara M, Brown DT, Hager GL, Latham K, Adashi EY, Misteli T. Differential in vivo binding dynamics of somatic and oocyte-specific linker histones in oocytes and during ES cell nuclear transfer. *Mol Biol Cell* 2005; 16:3887–3895.
32. Higashi T, Matsunaga S, Isobe K, Morimoto A, Shimada T, Kataoka S, Watanabe W, Uchiyama S, Itoh K, Fukui K. Histone H2A mobility is regulated by its tails and acetylation of core histone tails. *Biochem Biophys Res Commun* 2007; 357:627–632.
33. Kimura H. Histone dynamics in living cells revealed by photobleaching. *DNA Repair (Amst)* 2005; 4:939–950.
34. Mei J, Zhang QY, Li Z, Lin S, Gui JF. C1q-like inhibits p53-mediated apoptosis and controls normal hematopoiesis during zebrafish embryogenesis. *Dev Biol* 2008; 319:273–284.
35. Yin J, Xia JH, Du XZ, Liu J, Zhou L, Hong YH, Gui JF. Developmental expression of CagMdkb during gibel carp embryogenesis. *Int J Dev Biol* 2007; 51:761–769.
36. Thompson JD, Higgins DG, Gibson TJ. CLUSTAL W: improving the sensitivity of progressive multiple sequence alignment through sequence weighting, position-specific gap penalties and weight matrix choice. *Nucleic Acids Res* 1994; 22:4673–4680.
37. Pilch DR, Redon C, Sedelnikova OA, Bonner WM. Two-dimensional gel analysis of histones and other H2AX-related methods. *Methods Enzymol* 2004; 375:76–88.
38. Zhang X, Li X, Marshall JB, Zhong CX, Dawe RK. Phosphoserines on maize centromeric histone H3 and histone H3 demarcate the centromere and pericentromere during chromosome segregation. *Plant Cell* 2005; 17: 572–583.
39. Zhu R, Zhang YB, Zhang QY, Gui JF. Functional domains and the antiviral effect of the dsRNA-dependent protein kinase PKR from *Paralichthys olivaceus*. *J Virol* 2008; 82:6889–6901.
40. Xu H, Gui J, Hong Y. Differential expression of vasa RNA and protein during spermatogenesis and oogenesis in the gibel carp (*Carassius auratus gibelio*), a bisexually and gynogenetically reproducing vertebrate. *Dev Dyn* 2005; 233:872–882.
41. Ren Q, Gorovsky MA. The nonessential H2A N-terminus tail can function as an essential charge patch on the H2A.Z variant N-terminus tail. *Mol Cell Biol* 2003; 23:2778–2789.
42. White CL, Suto RK, Luger K. Structure of the yeast nucleosome core particle reveals fundamental changes in internucleosome interactions. *EMBO J* 2001; 20:5207–5218.
43. Shi Y, Zhang YB, Zhao Z, Jiang J, Zhang QY, Gui JF. Molecular characterization and subcellular localization of *Carassius auratus* interferon regulatory factor-1. *Dev Comp Immunol* 2008; 32:134–146.
44. Zhang YB, Jiang J, Chen YD, Zhu R, Shi Y, Zhang QY, Gui JF. The innate immune response to grass carp hemorrhagic virus (GCHV) in cultured *Carassius auratus* blastulae (CAB) cells. *Dev Comp Immunol* 2007; 31:232–243.
45. Kimura H, Hieda M, Cook PR. Measuring histone and polymerase dynamics in living cells. *Methods Enzymol* 2004; 375:381–393.
46. Phair RD, Gorski SA, Misteli T. Measurement of dynamic protein binding to chromatin in vivo, using photobleaching microscopy. *Methods Enzymol* 2004; 375:393–414.
47. Xia JH, Liu JX, Zhou L, Li Z, Gui JF. Apo-14 is required for digestive system organogenesis during fish embryogenesis and larval development. *Int J Dev Biol* 2008; 52:1089–1098.
48. Chambers AL, Downs JA. The contribution of the budding yeast histone H2A C-terminal tail to DNA-damage responses. *Biochem Soc Trans* 2007; 35:1519–1524.
49. Ausio J, Abbott DW. The many tales of a tail: carboxyl-terminal tail heterogeneity specializes histone H2A variants for defined chromatin function. *Biochemistry* 2002; 41:5945–5949.
50. Selman K, Wallace RA, Sarka A, Qi X. Stages of oocyte development in the zebrafish, *Brachydanio rerio*. *J Morphol* 1993; 218:203–224.
51. Teranishi T, Tanaka M, Kimoto S, Ono Y, Miyakoshi K, Kono T, Yoshimura Y. Rapid replacement of somatic linker histones with the oocyte-specific linker histone H1foo in nuclear transfer. *Dev Biol* 2004; 266:76–86.
52. Placke BJ, Gloss LM. Three-state kinetic folding mechanism of the H2A/H2B histone heterodimer: the N-terminal tails affect the transition state between a dimeric intermediate and the native dimer. *J Mol Biol* 2005; 345:827–836.
53. De La Fuente R. Chromatin modifications in the germinal vesicle (GV) of mammalian oocytes. *Dev Biol* 2006; 292:1–12.
54. Eilertsen KJ, Power RA, Harkins LL, Misica P. Targeting cellular memory to reprogram the epigenome, restore potential, and improve somatic cell nuclear transfer. *Anim Reprod Sci* 2007; 98:129–146.
55. Zhang Y, Griffin K, Mondal N, Parvin JD. Phosphorylation of histone H2A inhibits transcription on chromatin templates. *J Biol Chem* 2004; 279:21866–21872.
56. Barber CM, Turner FB, Wang Y, Hagstrom K, Taverna SD, Mollah S, Ueberheide B, Meyer BJ, Hunt DF, Cheung P, Allis CD. The enhancement of histone H4 and H2A serine 1 phosphorylation during mitosis and S-phase is evolutionarily conserved. *Chromosoma* 2004; 112: 360–371.
57. Sarcinella E, Zuzarte PC, Lau PN, Draker R, Cheung P. Monoubiquitylation of H2A.Z distinguishes its association with euchromatin or facultative heterochromatin. *Mol Cell Biol* 2007; 27:6457–6468.
58. Reik W, Santos F, Mitsuya K, Morgan H, Dean W. Epigenetic asymmetry in the mammalian zygote and early embryo: relationship to lineage commitment? *Philos Trans R Soc Lond B Biol Sci* 2003; 358:1403–1409.
59. Santos F, Peters AH, Otte AP, Reik W, Dean W. Dynamic chromatin modifications characterise the first cell cycle in mouse embryos. *Dev Biol* 2005; 280:225–236.
60. Henikoff S. Nucleosome destabilization in the epigenetic regulation of gene expression. *Nat Rev Genet* 2008; 9:15–26.
61. Luk E, Vu ND, Patteson K, Mizuguchi G, Wu WH, Ranjan A, Backus J, Sen S, Lewis M, Bai Y, Wu C. Chz1, a nuclear chaperone for histone H2AZ. *Mol Cell* 2007; 25:357–368.